Echo Canceller Based on Adaptive Interpolated FIR Filters

Orlando J. Tobias, Rui Seara Júnior, and Rui Seara
Federal University of Santa Catarina, Florianópolis SC, Brazil

Abstract - **In this paper, the use of adaptive interpolated FIR-LMS structures for echo cancelling in digital telephone systems is assessed. These structures are compared with the widely used FIR-LMS one. By using interpolated structures, it is possible to achieve substantial savings in the required arithmetic for both filtering and tap updating operations. Experimental results show that the interpolated structures also outperform, in terms of residual echo, the traditional FIR structure.**

I. INTRODUCTION

The most common implementation of adaptive echo cancellers is based on FIR-LMS filter structures [1-4]. A typical block diagram of an adaptive echo canceller is depicted in Fig. 1. The widespread use of FIR-LMS cancellers is mainly due to its simple implementation and stability. However, a major drawback of this structure for echo cancelling applications is the large number of taps required. For instance, to accommodate echoes of the order of 16-64 ms, at a sampling rate of 8 kHz, we need 512 taps. In acoustic echo cancellation this question becomes even more emphasized, usually demanding adaptive filters having several thousands of taps. In this sense, considerable research effort has been made to reduce the computational complexity of the echo cancellers, while maintaining a satisfactory echo reduction.

An interesting alternative to reduce the computational complexity in digital FIR filters is the use of interpolated FIR (IFIR) filters [5,6]. The basic idea behind the IFIR filters is to remove quite a few impulse response samples, and next, recreating them through an interpolating filter. Such a procedure leads to a less expensive implementation of FIR filters. In addition, IFIR filters possess all desirable properties of the FIR structures. In the same way, the adaptive version of IFIR (AIFIR) filters can be used to replace the classical adaptive FIR (AFIR) filters in applications in which a large number of taps are required [5-10]. The use of adaptive IFIR structures permits to reduce the number of arithmetic operations involved in both filtering and tap updating.

Orlando J. Tobias, Rui Seara Júnior, and Rui Seara are with LINSE: Circuits and Signal Processing Laboratory, Department of Electrical Engineering, Federal University of Santa Catarina, Florianópolis, SC, Brazil, 88040-900, Phone: +55 48 331 9643, Fax: +55 48 331 9091, E-mails: {orlando, ruijr, seara}@linse.ufsc.br.

In this work, an echo canceller using an ordinary FIR-LMS implementation is compared with an IFIR-LMS one for performance. For this comparison, real-world data, obtained from a digital telephone system, is used. Through the presented simulations, it is possible to verify that the interpolated structure outperforms the classical one.

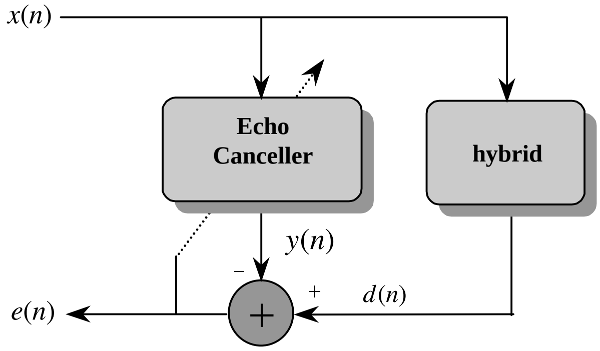

Fig. 1. Typical block diagram of an echo cancelling system.

II. INTERPOLATED FIR FILTER STRUCTURES

Based on the previous concept, a fixed interpolated filter is implemented by the series combination of two basic blocks [5,6]:

i) a sparse FIR filter;
ii) an interpolating FIR filter.

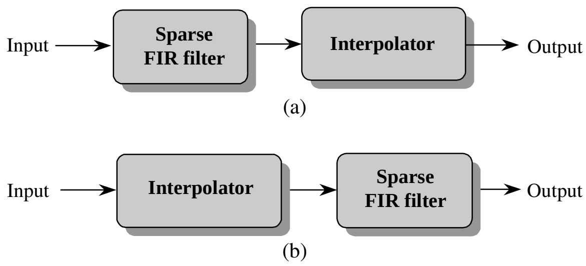

Fig. 2. IFIR filter. (a) Direct, and (b) Inverted structures.

In Fig. 2, the direct and inverted IFIR structures are shown. Such structures lead to a reduction in about $(1/L)$ the number of arithmetic operations when compared with the equivalent ordinary approach, where L represents the filter decimating factor. In other words, the sparse filter has $(L-1)$ zero-taps between two nonzero taps. Thus, the advantage of this structure becomes evident regarding the required number of computations to determine an output sample. In the next section, we discuss the implementation of the adaptive version of the structures of Fig. 2.

III. Weight Update Equations

Figure 3 depicts the block diagrams for the ordinary FIR-LMS and IFIR-LMS filters. In Fig. 3, $\mathbf{X}(n)=[x(n),x(n-1),\ldots,x(n-N+1)]^T$ and $d(n)$ represent the input vector (far signal) and echo to be cancelled, respectively. For Fig. 3(a), the well-known tap-update recursion (LMS algorithm [4]) is given by

$$\mathbf{W}_1(n+1)=\mathbf{W}_1(n)+2\mu e_1(n)\mathbf{X}(n), \tag{1}$$

where $\mathbf{W}_1(n)=[w_{10}(n),w_{11}(n),\ldots,w_{1,N-1}(n)]^T$ is the adaptive-tap vector; and $e_1(n)$ is the error signal obtained by

$$e_1(n)=d(n)-y_1(n)=d(n)-\mathbf{X}^T(n)\mathbf{W}_1(n)\,. \tag{2}$$

The tap-update expression for the IFIR-LMS direct structure, Fig. 3(b), is given by [11]

$$\mathbf{W}_2(n+1)=\mathbf{F}(\mathbf{W}_2(n)+2\mu e_2(n)\mathbf{X}_I(n)). \tag{3}$$

In (3), vector $\mathbf{X}_I(n)=[x_I(n),x_I(n-1),\ldots,x_I(n-N+1)]^T$ represents the filtered input signal (filtered far signal), where

$$x_I(n)=\sum_{j=0}^{M-1} i_j x(n-j) \tag{4}$$

and

$$\mathbf{X}_I(n)=\sum_{j=0}^{M-1} i_j \mathbf{X}(n-j)\,, \tag{5}$$

where i_j, with $j=0,\ldots,M-1$, represents the coefficients of the interpolating filter. Note that the block diagram of Fig. 3(b) corresponds to the filtered-X LMS algorithm [12]. In this way, to adapt the taps in an IFIR-LMS structure, instead of the classical LMS algorithm, the filtered version of this algorithm must be used. In addition, due to the sparse nature of the adaptive filter, the study of the adaptive IFIR filter needs to be carried out by using a constrained analysis. A detailed stochastic analysis of the IFIR-LMS filter is presented in [11]. Matrix $\mathbf{F}$ has the function of keeping the adaptive-tap vector sparse during the adaptation process. For this case, the error signal is given by

$$e_2(n)=d(n)-y_2(n)=d(n)-\sum_{j=0}^{M-1} i_j \mathbf{X}^T(n-j)\mathbf{W}_2(n-j)\,. \tag{6}$$

By commuting the adaptive and interpolator filters in Fig. 3(b) (assuming slow adaptation) [7,13], one obtains the following update equation

$$\mathbf{W}_3(n+1)=\mathbf{F}(\mathbf{W}_3(n)+2\mu e_3(n)\mathbf{X}_I(n)), \tag{7}$$

Matrix $\mathbf{F}$ in (7) has the same structure as in (3). From Fig. 3(c), the error signal in (7), is determined as follows

$$e_3(n)=d(n)-y_3(n)=d(n)-\sum_{j=0}^{M-1} i_j \mathbf{X}^T(n-j)\mathbf{W}_3(n)\,. \tag{8}$$

Notice, from (6) and (8), that the expressions for the error signals are different.

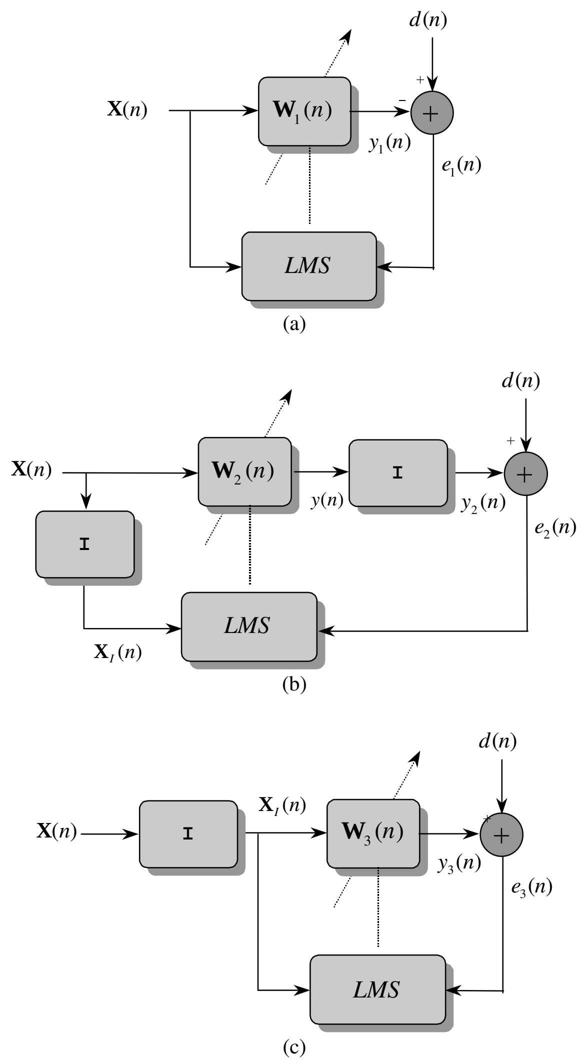

Fig. 3. (a) Classical FIR-LMS filter. IFIR-LMS filter: (b) direct; and (c) inverted structures.

A. Structure of Matrix F

In this section, we show how the matrix **F** is constructed. To this end, and without loss of generality, this is discussed through an example. Let us consider an adaptive filter with four taps and an interpolating factor (decimating factor) $L = 2$. This configuration leads to two taps to be adapted; while the remaining two are fixed to zero. The adaptive filter has the following form $\mathbf{W}(n) = [w_0(n), w_1(n), w_2(n), w_3(n)]$, however, according to previous conditions, one has $w_1(n) = w_3(n) = 0$. This results in that only the even taps are adapted. Thus, to fulfill the above condition, Matrix **F** must be [7,11]

$$\mathbf{F} = \begin{pmatrix} 1 & 0 & 0 & 0 \\ 0 & 0 & 0 & 0 \\ 0 & 0 & 1 & 0 \\ 0 & 0 & 0 & 0 \end{pmatrix}.$$

IV. Computational Complexity

The required number of computations in each iteration for both operations, filtering and tap updating, for the FIR-LMS and IFIR-LMS structures having N taps, are shown in Table I. For the sake of simplicity, the multiplication by the constant μ (step size) is not considered. Since the number of coefficients of the interpolator filter is very low (three coefficients in our implementation), the required arithmetic operations by the interpolating filter are also disregarded. Note that depending on the chosen interpolating factor (L), the IFIR-LMS structure can reduce in 50% ($L = 2$) the required computations. If, for instance, a value of $L = 3$ were used, we would obtain a computation saving of approximately 70%.

TABLE I
REQUIRED COMPUTATIONS FOR THE ADAPTIVE ALGORITHMS

Structure	Filtering		Updating		Total	
	+	×	+	×	+	×
Ordinary FIR-LMS	N	N	N	N	$2N$	$2N$
IFIR-LMS	N/L	N/L	N/L	N/L	$2(N/L)$	$2(N/L)$

V. Implementation Comments

In this section, we address the implementation of the filtering and tap-update operations of an IFIR-LMS structure for echo cancelling application. By considering the implementation cost and performance, the inverted structure was chosen (Fig. 3(c)). Note that it uses a single interpolator, instead of two as required by the direct form. Regarding the performance, in the experimental result section, it is verified that the inverted form outperforms the direct one. The tap-updating equation for the inverted form is given by the recursive expression (7). In our implementation, we have used $L = 2$. Thus, the implementation of the adaptive algorithm is summarized as follows:

i) define an adaptive vector with $N/2$ taps;
ii) determine $x_I(n)$: the filtered input is obtained by filtering the far signal through the interpolator;
iii) by storing $x_I(n)$ in an N-element circular buffer, the $\mathbf{X}_I(n)$ vector is created;
iv) echo estimate, $y_3(n)$: select the even samples from the circular buffer for creating an $N/2$-element filtered input vector, and next, perform the scalar product with the $N/2$-tap adaptive vector. This operation is equivalent to $\mathbf{X}_I^T(n)\mathbf{W}(n)$, where $\mathbf{X}_I(n)$ is an $N \times 1$ vector and $\mathbf{W}(n)$ is an $N \times 1$ sparse vector.
v) determine the error signal between the echo signal and its estimate;
vi) updating operation: the adaptive vector is updated by using the same element selection as in the step (iv).

Note that in fact, we are working with an $N \times 1$ input vector, from which we use only $N/2$ samples in our computations. The advantage of this is that we can cover echo duration corresponding to N-taps. An implementation of this echo cancelling structure has been carried out using a fixed-point Analog Devices digital signal processor (ADSP 218x family). By using $N = 128$ taps, an interpolating filter with 3 coefficients, and a sampling rate of 8 kHz, we have obtained a performance of 1.8 MIPS, in contrast with 3.3 MIPS resulting from an equivalent FIR-LMS implementation.

VI. Experimental Results

In this section we present simulation results comparing the classical FIR-LMS implementation (128 taps) with the two proposed IFIR-LMS structures for performance. For the interpolated structures, we use $L = 2$, resulting in 64 taps to be adapted. The used interpolator filter is $\mathbf{I} = [0.5, 1, 0.5]$. For our simulations the far and echo signals are real-world data, sampled at 8 kHz. The echo signal to be cancelled is depicted in Fig. 4. To obtain the fairest possible comparison, the step size μ for each adaptive canceller is selected to attain the minimum value for the variance of the echo residual. To this end, we raised the value of μ for each adaptive canceller until its maximum allowable value; i.e., beyond this value, the adaptive algorithm diverges. For the FIR-LMS and inverted IFIR-LMS cancellers, we have found $\mu_{\max} = 0.1$. Meanwhile, for the direct IFIR-LMS structure, $\mu_{\max} = 0.06$ has been obtained.

For each μ, we determine the ratio $\sigma^2_{echoresidual} / \sigma^2_{echo}$, the results are depicted in Fig. 5. From that figure, a better performance of the inverted IFIR-LMS structure, with respect to both the classical FIR-LMS and direct IFIR-LMS structures, can be observed. We attribute this behavior to the fact that in the inverted structure both the LMS algorithm and adaptive filter use a filtered version of the echo signal (see Fig. 3(c)). In this case, the interpolator filter also performs the task of line-noise reduction; hence, the system (adaptive filter and algorithm) deals with a cleaner signal. Note that such an improvement is achieved by using 50% of the number of taps of the classical FIR-LMS structure. In Fig. 6, a better echo tracking for the inverted IFIR-LMS structure can be verified, which is referred to the lower obtained residual echo. For clarity, in that figure, we have only plotted the curves corresponding to the inverted-IFIR-LMS and the FIR-LMS structures.

In order to maintain the original signal as unaltered as possible, the frequency response of the interpolator filter must be closely related to the signals involved in the current application. For instance, in our application (telephone systems with voice-band of 300 to 3400 Hz), the interpolator is a low-pass filter transparent for the voice-band spectrum. Design procedures for the interpolator filter can be found in [14].

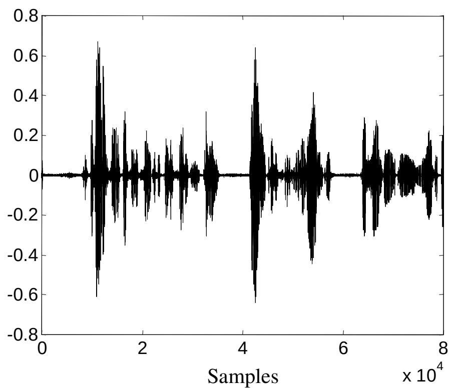

Fig. 4. Real-world echo signal containing 80.000 samples.

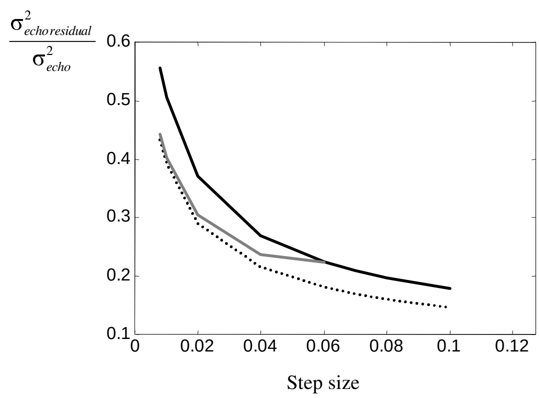

Fig. 5. Relative echo variance against step size. Dark line: ordinary FIR-LMS; gray line: direct IFIR-LMS; and dotted line: inverted IFIR-LMS structures.

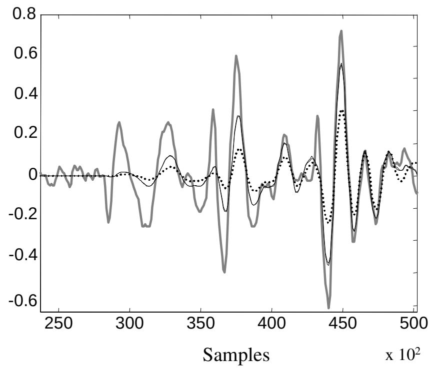

Fig. 6. Echo signal and its estimates. Gray line: original echo signal; dotted lines and solid-dark: echo estimates from FIR-LMS and inverted IFIR-LMS cancellers, respectively.

VII. CONCLUSIONS

Two IFIR-LMS structures for echo cancelling application are compared with the classical FIR-LMS one. The computational complexity reduction, tracking characteristics as well as the residual echo level of the adaptive interpolated structures are addressed. Extensive simulations with real-world data have been carried out to perform comparisons between the studied structures. From these, we can verify a better performance of the interpolated structures, in particular its inverted form, for echo cancelling in digital voice-transmission applications.

REFERENCES

[1] M. M. Sondhi and D. A. Berkley, "Silencing echoes on the telephone network," *Proceedings of the IEEE*, vol. 68, no. 8, pp. 948-963, Aug. 1980.

[2] D. J. Messerschmitt, "Echo cancellation in speech and data transmission," *IEEE J. Selected Areas Comm.*, vol. SAC-2, pp. 283-297, Nov. 1983.

[3] M. L. Honig, "Echo cancellation of voiceband data signals using recursive least squares and stochastic gradient algorithms," *IEEE Trans. on Communications*, vol. COM-33, pp. 65-73, Jan. 1985.

[4] S. Haykin, *Adaptive Filter Theory*, Prentice-Hall, NJ, 1996.

[5] Y. Neuvo, C. Y. Dong and S. K. Mitra, "Interpolated finite impulse response digital filters," *IEEE Trans. Acoust., Speech, Signal Processing*, vol. ASSP-32, pp. 563-570, Jun. 1984.

[6] Y. Neuvo, G. Rajan and S. K. Mitra, "Design of narrow-band FIR bandpass digital filters with reduced arithmetic complexity," *IEEE Trans. Circuits Syst.*, vol. 34, pp. 409-419, Apr. 1987.

[7] R. Seara, J. C. M. Bermudez and E. Beck, "A new technique for the implementation of adaptive IFIR filters," *Proc. ISSSE'92*, Paris, France, pp. 644-647, 1992.

[8] A. Abousaada, T. Aboulnasr and W. Steenaart, “An echo tail canceller based on adaptive interpolated FIR Filtering,” *IEEE Trans. Circuits Syst.-II*, vol. 39, pp. 409-416, Jul. 1992.

[9] J. E. Greenberg, “Modified LMS algorithms for Speech processing with an adaptive noise canceller,” *IEEE Trans. on Speech and Audio Process.*, vol. 6, pp. 338-351, Jul. 1998.

[10] A. P. Liavas and P. A. Regalia, “Acoustic echo cancellation: Do IIR models offer better modeling capabilities than their FIR counterparts?,” *IEEE Trans. on Signal Process.*, vol. 46, pp. 2499-2504, Sept. 1998.

[11] O. J. Tobias and R. Seara, “Analytical model for the first and second moments of an adaptive interpolated FIR filter using the constrained filtered-X LMS algorithm,” *IEE Proceedings – Vision, Image and Signal Processing*, vol. 148, pp. 337-346, Oct. 2001.

[12] O. J. Tobias, J. C. M. Bermudez and N. Bershad, “Mean weight behavior of the Filtered-X LMS algorithm,” *IEEE Trans. on Signal Processing*, vol. 48, no. 4, pp. 1061-1075, Apr. 2000.

[13] O. J. Tobias, R. Seara and C. A. F. Rocha, “Analytical model for the mean weights of two adaptive interpolated-FIR filter structures,” *Proc. 2000 IEEE Int. Symp. Circuits Systems*, Geneva, Switzerland, pp. III.93-III.96, May 2000.

[14] T. Saramäki, Y. Neuvo and S. K. Mitra, “Design of computationally efficient interpolated FIR filters,” *IEEE Trans. Circuits and Systems*, vol. 35, pp. 70-88, Jan. 1988.